International Journal of Power Electronics and Drive System (IJPEDS)
Vol. 7, No. 4, December 2016, pp. 1061~1074
ISSN: 2088-8694, DOI: 10.11591/ijpeds.v7i4.pp1061-1074

Sensorless Control of a Fault Tolerant PMSM Drives in Case of Single-phase Open Circuit Fault

Kamel Saleh[1], Mark Sumner[2]
[1] Department of Electrical Engineering, An-Najah National University, Palestine
[2] Department of Electrical Engineering, Nottingham University, United Kingdom

Article Info

Article history:

Received May 22, 2016
Revised Oct 26, 2016
Accepted Nov 7, 2016

Keyword:

Case of single-phase fourth
Circuit fault
Fault tolerant PMSM drives
Sensorless control

ABSTRACT

This paper introduces a sensorless-speed-controlled PMSM motor fed by a four-leg inverter in case of a single phase open circuit fault regardless in which phase is the fault. To minimize the system performance degradation due to a single phase open circuit fault, a fault tolerant control strategy that includes taking appropriate actions to control the two remaining healthy currents is used in addition to use the fourth leg of the inverter. Tracking the saliency is done through measuring the dynamic current responses of the healthy phases of the PMSM motor due the IGBT switching actions using the fundamental PWM method without introducing any modification to the operation of the fourth leg of the inverter. Simulation results are provided to verify the effectiveness of the proposed strategy for sensorless controlling of a PMSM motor driven by a fault-tolerant four-phase inverter over a wide speed ranges under the case of a single phase open circuit.

Corresponding Author:

Kamel Saleh,
Department of Electrical and Computer Engineering,
An-Najah National University, Nablus, West Bank, Palestine.
Email: kamel.saleh@najah.edu

1. INTRODUCTION

Many techniques for tracking the saliency of a healthy ac motor fed by three-leg inverter at low speed have been researched such as the injection of high frequency voltage [1-3] or the injection of test pulses [4-6]. Those techniques give good results for sensorless speed-controlled healthy (ie no faults) motors even at zero speed and full load. In some applications such that in the coiling and spooling textile machines and that of the aerospace and automotive (electric cars) industry, the safety procedures extremely demands a continued operation of the motor drive system after a fault has occurred to reduce the impact of the fault on the system operation. And hence, number of fault-tolerant strategies for sensored ac motor drives have been used to enhance the system operation under open phase fault. The fault-tolerant strategies proposed in [7-9] are based on the connection of either the stator windings neutral point or the motor phase to the dc link middle point of the two level three–leg inverter through a triac. The authors of [10] proposed a two level four-leg inverter where the fourth leg is connected to the neutral point of the motor in the case of open circuit phase fault. In [11], the fourth leg is connected to the neutral point in healthy and faulty cases and so 3D space vector modulation is introduced. The authors of [12] proposed the switching function algorithm for a four-leg converter to synthesize redefined output waveforms under fault condition. In [13], a new starategy to track the saliency in a fault-tolerant inverter in case of single phase open circuit in phase ‘a’ only has been proposed.

This paper proposes a fault-tolerant, four-phase inverter PMSM drive topology which can be used to track the saturation saliency in PM motors and rotor slotting saliency in induction motors in the case of a single phase open circuit fault regardless in which phase is the fault in order to maintain a continues system

operation with a satisfactory performance to meet the safety procedures for the whole system and to increase the reliability of the system.

2. RESEARCH METHOD

2.1 Fault-Tolerant Two Level Four-Leg Converter Drive Topology

Figure 1 shows the proposed faul-tolerant two level four-leg converter drive topology [14-20]. In this topology, a fourth leg is added to the conventional three-leg inverter and the redundant leg is permanently connected the motor neutral point to provide a fault-tolerant capability in case of an open phase fault. Under healthy operating conditions, the fourth-leg will be redundant which means that the two switches in this leg will be inactivated resulting in no connection between the supply and the motor neutral point. Therefore, the proposed converter normally operates as a conventional two-level three-leg inverter. In case of an open circuit fault in one phase, the switches on the faulty phase are disabled and the switches in the fourth phase are immediately activated in order to control the voltage at the neutral point of motor.

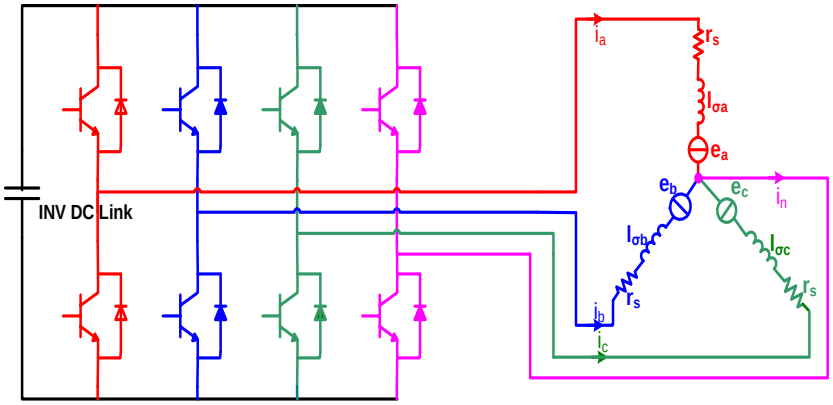

Figure 1. The fault-Tolerant Two Level Four-Leg Converter Motor Drive Configuration

2.2 Sensored Control Strategy for the Fault Tolerant Motor Drive

Indirect vector control is employed to control the speed of the motor in both normal and faulted operating conditions.

2.2.1 Normal Operating Condition in Sensored Mode

Figure 2 shows the vector control structure used for the two level four-leg inverter motor drive working under healthy conditions in sensored mode. The three currents of the motor are transformed to the d-q synchronous rotating frame, id and iq, as given in (1) to be compared with the reference values. The reference voltages (Vd and Vq) generated from the controller are transformed back using equation 2 to three phase quantities which then delivered to the space vector modulator to generate the appropriate switching signals for the fault-tolerant inverter switches.

$$\begin{bmatrix} Iq \\ Id \\ I0 \end{bmatrix} = \frac{2}{3}\begin{bmatrix} \cos(\theta) & \cos(\theta-120) & \cos(\theta+120) \\ \sin(\theta) & \sin(\theta-120) & \sin(\theta+120) \\ 0.5 & 0.5 & 0.5 \end{bmatrix}\begin{bmatrix} Ia \\ Ib \\ Ic \end{bmatrix} \quad (1)$$

$$\begin{bmatrix} Va \\ Vb \\ Vc \end{bmatrix} = \begin{bmatrix} \cos(\theta) & \sin(\theta) & 1 \\ \cos(\theta-120) & \sin(\theta-120) & 1 \\ \sin(\theta-120) & \sin(\theta+120) & 1 \end{bmatrix}\begin{bmatrix} Vq \\ Vd \\ V0 \end{bmatrix} \quad (2)$$

where θ is the rotor angle of the reference frame. I0 is the zero sequence current while In is the motor neutral current as expressed in equations (1) and (2), respectively. Under normal operating conditions, the neutral current is always zero.

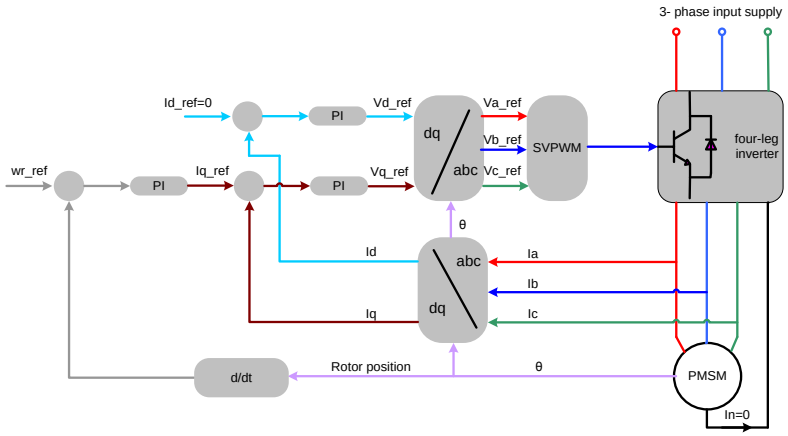

Figure 2. Control Structure of Four-Leg PMSM Drive under Healthy Operating Conditions

2.2.2 Open Phase Fault Operation

In order to keep the performance of the motor in case of an open circuit fault condition as good as that of the healthy motor, the rotating MMF obtained from the stator currents (Ia,Ib,Ib) in healthy conditions, should be maintained by the two remaining motor currents in the case of an open circuit fault condition. This demands an increasing of the two remaining currents of the motor by $\sqrt{3}$ as well as phase shifting by 30 degrees away from the faulted phase as given in equation 3.

$$\begin{bmatrix} I0 \\ Ib \\ Ic \end{bmatrix} = \begin{bmatrix} -\cos(\theta) & -\sin(\theta) \\ \sqrt{3}\cos(\theta - 150) & \sqrt{3}\sin(\theta - 150) \\ \sqrt{3}\sin(\theta - 150) & \sqrt{3}\sin(\theta + 150) \end{bmatrix} \begin{bmatrix} Vq \\ Vd \end{bmatrix} \quad (3)$$

To do that, a modification is introduced to the control strategy of the system in case of an open phase fault condition as illustrated [14-20]. The reference volateg of the faulty phase is set to zero and at the same time the switching in the fourth leg of the inverter is activated such that the neutral, which is the sum of the two remaining output currents, can circulate. Figure 3 shows the vector control structure for the four-leg inverter PMSM drive under a phase ‘c’ open circuit fault as an example. Vc_ref is set to zero also ic is set to zero and the switching of the fourth leg is activated. If the fault occurs in phase b or phase a, similar proecedures will be implemented.

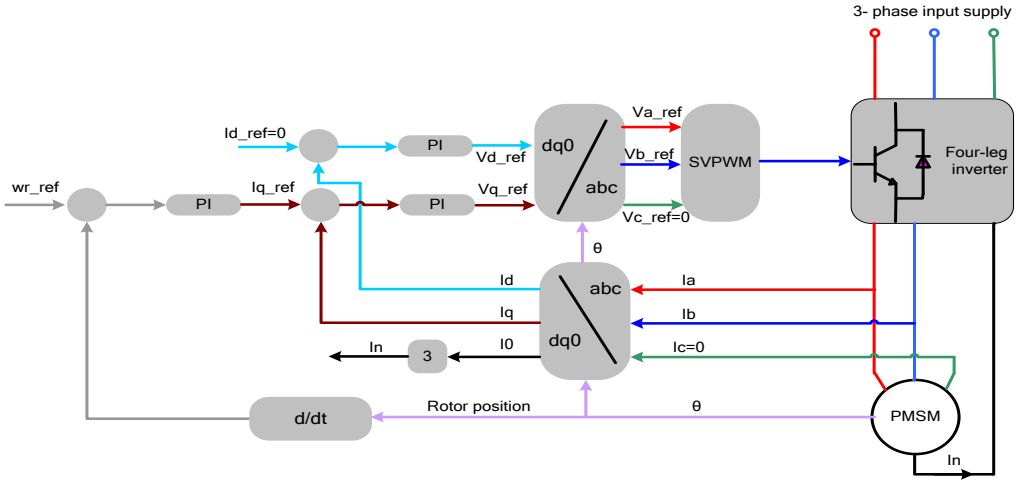

Figure 3. The Vector Control Structure for the Four-Leg Inverter PMSM Drive under a Phase 'C' Open-Circuit Fault

2.3 Simulation Results

The simulation of four-leg inverter PMSM drive has been carried out using SABER. A 10 Nm load torque and a 120 rpm speed command are applied to the system. Figure 4 shows the simulation results of the four-leg inverter PMSM drive system under healthy and faulty conditions. The motor was running at 120 rpm in helathy conditions then a phase 'a' open circuit fault is introduced to the operation of the motor between 3s and 4s, after that, the fault in phase 'a' is removed and the motor returns to a healthy operating conditions between times 4s and 5s. Between times 5s and 6s a phase 'b' open circuit fault is introduced to the operation of the motor and again the fault is removed between times 6s and 7s. Finally, a fault in phase 'c' is introduced between times 7s and 8s. Under each faulty condition, the control strategy mentioned in previous section is applied. It is clear that the controller could regulate the motor speed to follow the reference speed properly under normal operating condition and faulty conditions. The controlled currents id and iq are stable at the reference levels regardless whether the motor currents are balanced three-phase sinusoidal (healthy condition) or unbalanced 2 phase sinusoidal currents (fault condition). Also it can be seen that I0 is equal to zero while the motor is working in healthy conditions (fourth leg is deactivated) and when the fault condition is happened, it will start to flow by activating the fourth leg. The simulation results shows that control stategy that is adopted in this work is succeed keep the performance of the system in faulty conditions as good as that in helathy conditions.

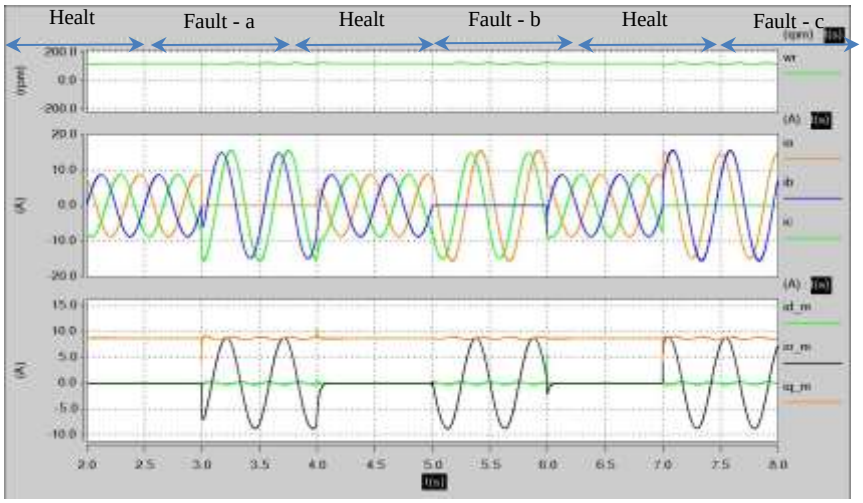

Figure 4. Performance of a Four-Leg Inveter PMSM Drive System Under Different Operating Conditions

2.4 Tracking the Saturation Saliency of PMSM under Healthy Condition

The stator leakage inductances of the induction motor are modulated by anisotropy either from the rotor slotting or from the saturation of the main flux. The modulation can be expressed by the following equations:

$$l\sigma a = L_0 + \Delta L cos(n_{an}\theta_{an}) \quad (4)$$

$$l\sigma b = L_0 + \Delta L cos\left(n_{an}(\theta_{an} - \frac{2\pi}{3}\right) \quad (5)$$

$$l\sigma c = L_0 + \Delta L cos\left(n_{an}(\theta_{an} - \frac{4\pi}{3}\right) \quad (6)$$

Where L_0 is the average inductance and ΔL is the variation of leakage inductance due to the rotor anisotropy (n_{an}= 2 for saturation anisotropy).

This modulation of the stator leakage inductances will be reflected in the transient response of the motor line current to the test vector imposed by the inverter. So by using the fundamental PWM wave form and by measuring the transient current response to the active vectors it is possible to detect the inductance variation and track the rotor position as shown in [6] for three-leg inverter. Figure 5a, Figure 5b and Table 1 illustrate this method.

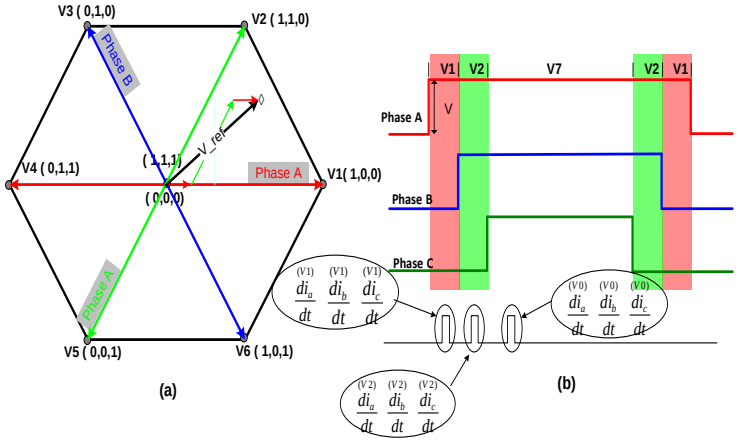

Figure 5. SVPWM Modulation Technique of 3-Leg Inverter in Healthy Mode: (a) Definition of Space Vectors; (b) Switching Patterns (Waveforms) in the First Sector

Table 1. Selection of Pa, Pb and Pc in Six Sectors for a Star-Connected Machine using Fundamental PWM Method

	P_a	P_b	P_c
V1+V0	$2-c(\frac{di_a}{dt}^{(V1)}-\frac{di_a}{dt}^{(V0)})$	$-1-c(\frac{di_c}{dt}^{(V1)}-\frac{di_c}{dt}^{(V0)})$	$-1-c(\frac{di_b}{dt}^{(V1)}-\frac{di_b}{dt}^{(V0)})$
V2+V0	$-1+c(\frac{di_b}{dt}^{(V2)}-\frac{di_b}{dt}^{(V0)})$	$-1+c(\frac{di_a}{dt}^{(V2)}-\frac{di_a}{dt}^{(V0)})$	$2+c(\frac{di_c}{dt}^{(V2)}-\frac{di_c}{dt}^{(V0)})$
V3+V0	$-1-c(\frac{di_c}{dt}^{(V3)}-\frac{di_c}{dt}^{(V0)})$	$2-c(\frac{di_b}{dt}^{(V3)}-\frac{di_b}{dt}^{(V0)})$	$-1-c(\frac{di_a}{dt}^{(V3)}-\frac{di_a}{dt}^{(V0)})$
V4+V0	$2+c(\frac{di_a}{dt}^{(V4)}-\frac{di_a}{dt}^{(V0)})$	$-1+c(\frac{di_c}{dt}^{(V4)}-\frac{di_c}{dt}^{(V0)})$	$-1+c(\frac{di_b}{dt}^{(V4)}-\frac{di_b}{dt}^{(V0)})$
V5+V0	$-1-c(\frac{di_b}{dt}^{(V5)}-\frac{di_b}{dt}^{(V0)})$	$-1-c(\frac{di_a}{dt}^{(V5)}-\frac{di_a}{dt}^{(V0)})$	$2-c(\frac{di_c}{dt}^{(V5)}-\frac{di_c}{dt}^{(V0)})$
V6+V0	$-1+c(\frac{di_c}{dt}^{(V6)}-\frac{di_c}{dt}^{(V0)})$	$2+c(\frac{di_b}{dt}^{(V6)}-\frac{di_b}{dt}^{(V0)})$	$-1+c(\frac{di_a}{dt}^{(V6)}-\frac{di_a}{dt}^{(V0)})$

After obtaing the scalar quantities Pa, Pb and Pc then the position of the saliency can be constructed as shown in the equation below:

$$\vec{p} = p_\alpha + jp_\beta = p_a + ap_b + a^2 p_c \quad (7)$$

For four leg-inverter, in time intervals 2s to 3s, 4s to 5s and 6s to 7s (helathy conditions) the switches in the fourth leg will not be activated so the algorithm proposed in [6] to track the saliency for three-leg inverter PMSM drive system can be applied for the four-leg inverter PMSM drive system as shown in Figure 6. In interval 3s to 4s (open phase fault in phase a), the measurement of the current response (dia/dt) will become zero i.e $\frac{di_a}{dt}^{V1}, \frac{di_a}{dt}^{V2}, \frac{di_a}{dt}^{V3}, \frac{di_a}{dt}^{V4}, \frac{di_a}{dt}^{V5}$ *and* $\frac{di_a}{dt}^{V0}$ become zeros as ia = 0. And so the position estimation algorithm couldn't track the saliency in this time interval. Aslo between 5s and 6s (open phase fault in phase b) and between 7s to 8s (open phase fault in phase c) the measurements of the current responces dib/dt and dic/dt will become zeros and hence the algorithm could't track the saliency in those time intervals as shown in Figure 6.

2.5 Tracking the Saturation Saliency of PMSM under Helathy and Unhealthy Condition

As seen in previous section, the algorithm presented in [6] to track the saliency in helathy condition can't be used under the case of phase open circuit fault. In this section a modified algorithm that make use of the switching action of the IGBTs in the fourth leg of the inverter to track the saliency in the case of open circuit fault case using the current response of application of fundamental PWM waveform (no modification applied to the PWM waveform). The new algorithm uses only the current response of application of fundamental PWM wave form of healthy phases to track the saliency and doesn't use the current response of the open circuit phase as it will be zero. After measuring the current response of the two healthy phases and according to the sector number of the space vector modulation state diagram that the reference voltage exist in, the three position scalars quantities can be deduce and hence the saliency position can be optained.

Figure 7a and Figure 7b show the space vector modulation state diagram for 4-leg inverter in case of open circuit phase fault case. If V_ref exists in first sector, then the switching sequences and the timing of the applied vectors will be as shown in Figure 7b.

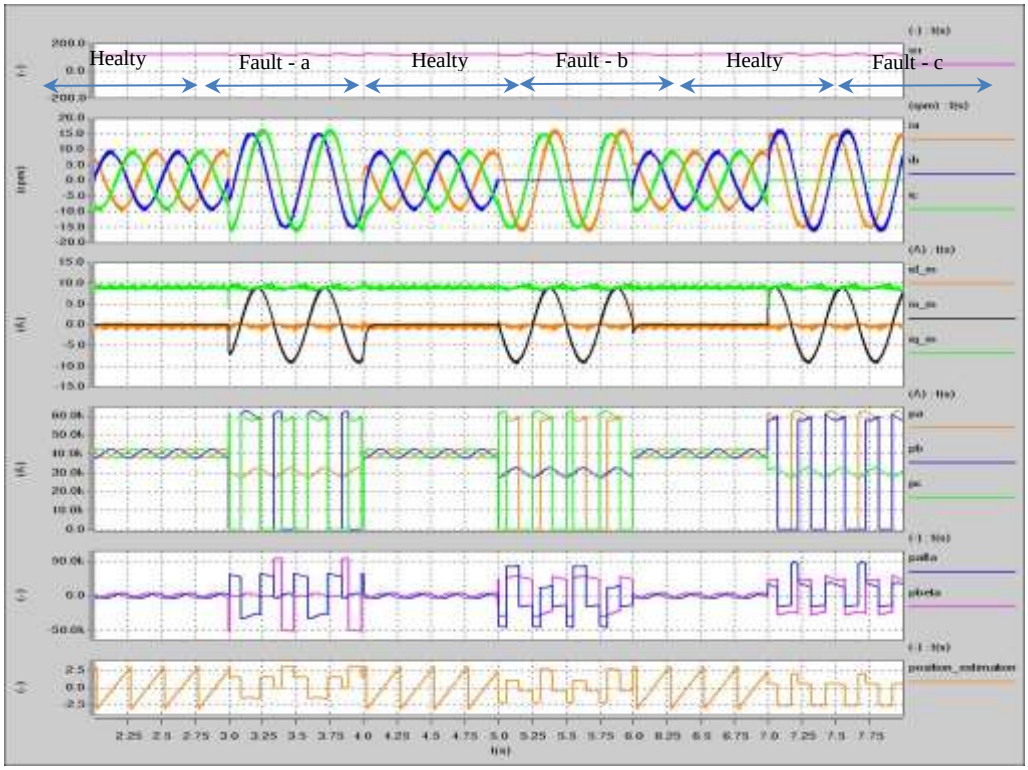

Figure 6. Tracking the Saliency Saturation in Healthy Mode and Phase a Open Circuit Case

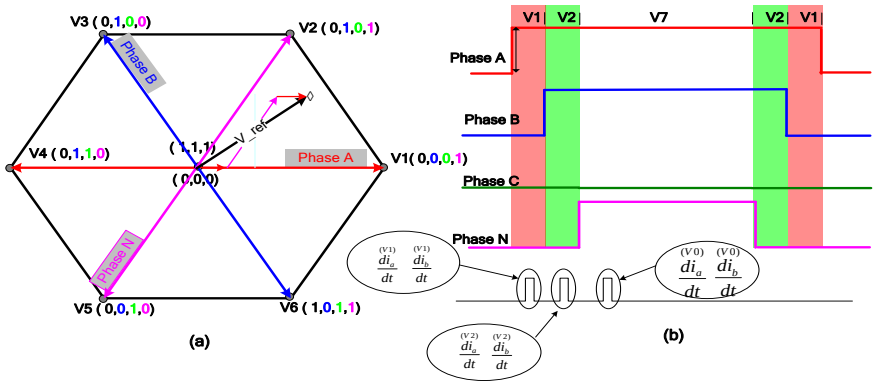

Figure 7. SVPWM modulation technique in phase c open circuit fault case: (a) definition of space vectors; (b) switching patterns (waveforms) in the first sector

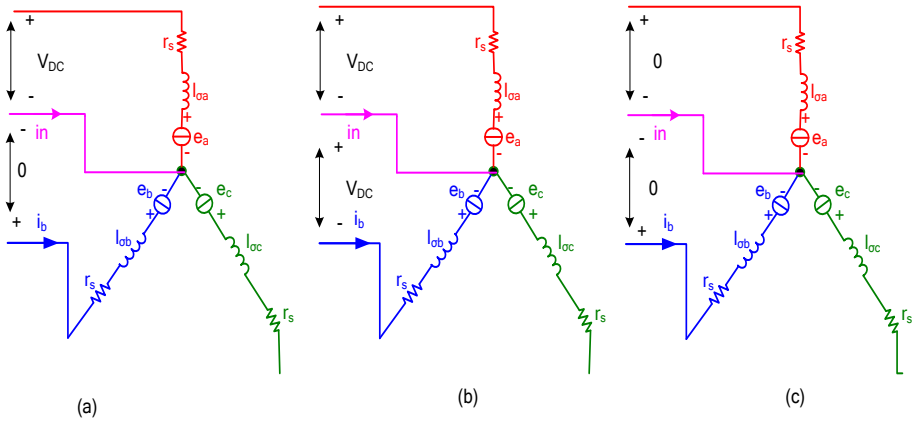

Figure 8. Stator Circuits When: (a) V1 is applied; (b) V2 is applied; (c) V0 is applied under phase c open circuit fault

The stator circuit when the vectors V1, V2 and V0 are applied are shown in Figures 8a, Figure 8b and Figure 8c respectively. Using the circuit in Figure 8a, the following equations hold true:

$$V_{DC} = r_s * i_a{}^{(V1)} + l_{\sigma a} * \frac{di_a^{(V1)}}{dt} + e_a^{(V1)} \quad (8)$$

$$V_{DC} = r_s * i_b{}^{(V1)} + l_{\sigma b} * \frac{di_b^{(V1)}}{dt} + e_b^{(V1)} V_{DC} \quad (9)$$

The following equations are obtained using Figure 8b:

$$V_{DC} = r_s * i_a{}^{(V2)} + l_{\sigma a} * \frac{di_a^{(V2)}}{dt} + e_a^{(V2)} \quad (10)$$

$$V_{DC} = r_s * i_b{}^{(V2)} + l_{\sigma b} * \frac{di_b^{(V2)}}{dt} + e_b^{(V2)} V_{DC} \quad (11)$$

Finally when V0 is applied as shown in Figure 8c, the following equations hold true:

$$0 = r_s * i_a{}^{(V0)} + l_{\sigma a} * \frac{di_a^{(V0)}}{dt} + e_a^{(V0)} \quad (12)$$

$$0 = r_s * i_b{}^{(V0)} + l_{\sigma b} * \frac{di_b^{(V0)}}{dt} + e_b^{(V0)} V_{DC} \quad (13)$$

Assuming that the voltage drop across the stator resistances are small and can be neglected and the back emf can be cancelled if the time separation between the vectors is small. Subtracting equations (12, 9) from equations (8, 11) respectively yields:

$$V_{DC} = l_{\sigma a} * \left(\frac{di_a^{(V1)}}{dt} - \frac{di_a^{(V0)}}{dt} \right) \quad (14)$$

$$V_{DC} = l_{\sigma b} * \left(\frac{di_b^{(V2)}}{dt} - \frac{di_b^{(V1)}}{dt} \right) \quad (15)$$

Finally

$$Pb = \left(\frac{di_a^{(V1)}}{dt} - \frac{di_a^{(V0)}}{dt} \right) \quad (16)$$

$$Pc = \left(\frac{di_b^{(V2)}}{dt} - \frac{di_b^{(V1)}}{dt}\right) \quad (17)$$

Pc can't be obtained from measuring the current response in phase c as it is zero in the case of open circuit phase. But it can be deduced from Pa and Pb according to the following equation:

$$Pc = -Pb-Pa \quad (18)$$

For the other sectors, the same priciples can be applied as shown in Table 2

Table 2. Selection of Pa, Pb and Pc for a Star-Connected Machine in case of a phase 'c'Open Circuit Fault

	Phase 'c' open circuit fault		
	P_a	P_b	P_c
V1+V2+V0	$(\frac{di_a}{dt}^{(V1)} - \frac{di_a}{dt}^{(V0)})$	$(\frac{di_b}{dt}^{(V2)} - \frac{di_b}{dt}^{(V1)})$	$-P_a - P_b$
V2+V3+V0	$(\frac{di_a}{dt}^{(V2)} - \frac{di_a}{dt}^{(V3)})$	$(\frac{di_b}{dt}^{(V3)} - \frac{di_b}{dt}^{(V0)})$	$-P_a - P_b$
V3+V4+V0	$(\frac{di_a}{dt}^{(V0)} - \frac{di_a}{dt}^{(V4)})$	$(\frac{di_b}{dt}^{(V3)} - \frac{di_b}{dt}^{(V0)})$	$-P_a - P_b$
V4+V5+V0	$(\frac{di_a}{dt}^{(V0)} - \frac{di_a}{dt}^{(V4)})$	$(\frac{di_b}{dt}^{(V4)} - \frac{di_b}{dt}^{(V5)})$	$-P_a - P_b$
V5+V6+V0	$(\frac{di_a}{dt}^{(V6)} - \frac{di_a}{dt}^{(V5)})$	$(\frac{di_b}{dt}^{(V0)} - \frac{di_b}{dt}^{(V6)})$	$-P_a - P_b$
V6+V1+V0	$(\frac{di_a}{dt}^{(V1)} - \frac{di_a}{dt}^{(V0)})$	$(\frac{di_b}{dt}^{(V0)} - \frac{di_b}{dt}^{(V6)})$	$-P_a - P_b$

The equations to track the saliency if the open circuit fault is in phase a or phase b can be obtained in the same way as given in Table 3 and Table 4 respectively.

Table 3. Selection of Pa, Pb and Pc for a Star-Connected Machine in case of a phase 'a' Open Circuit Fault

	Phase 'a' open circuit fault		
	P_a	P_b	P_c
V1+V2+V0	$-P_b - P_c$	$(\frac{di_b}{dt}^{(V2)} - \frac{di_b}{dt}^{(V1)})$	$(\frac{di_c}{dt}^{(V0)} - \frac{di_c}{dt}^{(V2)})$
V2+V3+V0	$-P_b - P_c$	$(\frac{di_b}{dt}^{(V3)} - \frac{di_b}{dt}^{(V0)})$	$(\frac{di_c}{dt}^{(V0)} - \frac{di_c}{dt}^{(V2)})$
V3+V4+V0	$-P_b - P_c$	$(\frac{di_b}{dt}^{(V3)} - \frac{di_b}{dt}^{(V0)})$	$(\frac{di_c}{dt}^{(V4)} - \frac{di_c}{dt}^{(V3)})$
V4+V5+V0	$-P_b - P_c$	$(\frac{di_b}{dt}^{(V4)} - \frac{di_b}{dt}^{(V5)})$	$(\frac{di_c}{dt}^{(V5)} - \frac{di_c}{dt}^{(V0)})$
V5+V6+V0	$-P_b - P_c$	$(\frac{di_b}{dt}^{(V0)} - \frac{di_b}{dt}^{(V6)})$	$(\frac{di_c}{dt}^{(V5)} - \frac{di_c}{dt}^{(V0)})$
V6+V1+V0	$-P_b - P_c$	$(\frac{di_b}{dt}^{(V0)} - \frac{di_b}{dt}^{(V6)})$	$(\frac{di_c}{dt}^{(V6)} - \frac{di_c}{dt}^{(V1)})$

Table 4. Selection of Pa, Pb and Pc for a Star-Connected Machine in case of a phase 'b'open circuit fault

	Phase 'b' open circuit fault		
	P_a	P_b	P_c
V1+V2+V0	$(\frac{di_a^{(V1)}}{dt} - \frac{di_a^{(V0)}}{dt})$	-P_a - P_c	$(\frac{di_c^{(V0)}}{dt} - \frac{di_c^{(V2)}}{dt})$
V2+V3+V0	$(\frac{di_a^{(V2)}}{dt} - \frac{di_a^{(V3)}}{dt})$	-P_a - P_c	$(\frac{di_c^{(V0)}}{dt} - \frac{di_c^{(V2)}}{dt})$
V3+V4+V0	$(\frac{di_a^{(V0)}}{dt} - \frac{di_a^{(V4)}}{dt})$	-P_a - P_c	$(\frac{di_c^{(V4)}}{dt} - \frac{di_c^{(V3)}}{dt})$
V4+V5+V0	$(\frac{di_a^{(V0)}}{dt} - \frac{di_a^{(V4)}}{dt})$	-P_a - P_c	$(\frac{di_c^{(V5)}}{dt} - \frac{di_c^{(V0)}}{dt})$
V5+V6+V0	$(\frac{di_a^{(V6)}}{dt} - \frac{di_a^{(V5)}}{dt})$	-P_a - P_c	$(\frac{di_c^{(V5)}}{dt} - \frac{di_c^{(V0)}}{dt})$
V6+V1+V0	$(\frac{di_a^{(V1)}}{dt} - \frac{di_a^{(V0)}}{dt})$	-P_a - P_c	$(\frac{di_c^{(V6)}}{dt} - \frac{di_c^{(V1)}}{dt})$

3. RESULTS AND ANALYSIS

3.1 Position Estimation in Sensored Mode

Figure 9 shows the results of the simulation after modifying the tracking saliency algorithm as in Table 2, Table 3 and Table 4 in faulty conditions. Between 2s and 3s, 4s and 5s, 6s and 7s, the motor was working in healthy conditions and hence the algorithim give in Table 1 [6] could track the saliency. Between times 3s and 4s (fault in phase 'a') the algorithm given in Table 3 is used to track the saliency. Between times 5s and 6s (fault in phase 'b') the algorthim given in Table 3 is used to track the saliency. Finally, between 7s and 7.5s (fault in phase 'c') the algorithim given in Table 1 is used to track the saliency. Figure 9 shows the effectiveness of the saliency tracking algorithm under the case of single phase fault condition regardless of which phase is the fault. It is worth to mention here that the differences in DC gain between healthy and unhealthy conditions in position scalars Pa,Pb and Pc is come from the way these position scalars are calculated and it is removed when alfa (palfa) and beta (pbeta) components of the position are calculated as shown in Figure 9.

3.2 Fully Sensorless Speed Control

A speed control for a PM machine has been simulated in the Saber modeling environment. The estimated position signals palfa and pbeta are used as the input to a mechanical observer [18] to obtain the the estimated speed signal $\omega^{\wedge}$ and a cleaned estimated position signal $\theta^{\wedge}$. Note that the simulation includes a minimum pulsewidth of 10us when di/dt measurements are made similar to experimental results of [6]. This estimated speed $\omega^{\wedge}$ and position $\theta^{\wedge}$are used to obtain a sensorless speed control as shown in Figure 10.

3.2.1 Low Speed Operation

Figure 11 shows the results of a fully sensorless speed control of a PMSM motor driven by a four-leg inverter at load using the algorithm proposed in [6] for the healthy case and the method proposed above in the case of an open circuit fault condition. The motor was working in sensorless healthy mode at speed=0.5 Hz then at time t=4 s an open circuit fault in phase 'a' is introduced to the system. The motor maintained its performance after the fault. At t=6s a speed step change from 0.5 Hz to 0 Hz is applied to the system while the motor was under open circuit fault in phase 'a'. Figure 11 shows that the motor responded to the speed step with a good transient and steady state response. When t=8s, the fault in phase 'a' is removed and introduced to phase 'b', Figure 11 shows the motor was tracking the zero reference speed during this time. At t=12s, the fault is removed from phase 'b' and introduced to phase 'c'. After that, when t=14s, a speed step change from 0 rpm to -0.5 Hz is applied to the system while the motor was working under open circuit fault in phase 'c'. Figure 11 shows that the motor responded to the speed step with good transient and steady state response. Finally, at t=16s, all the faults are removed and the motor returns to healthy condition.

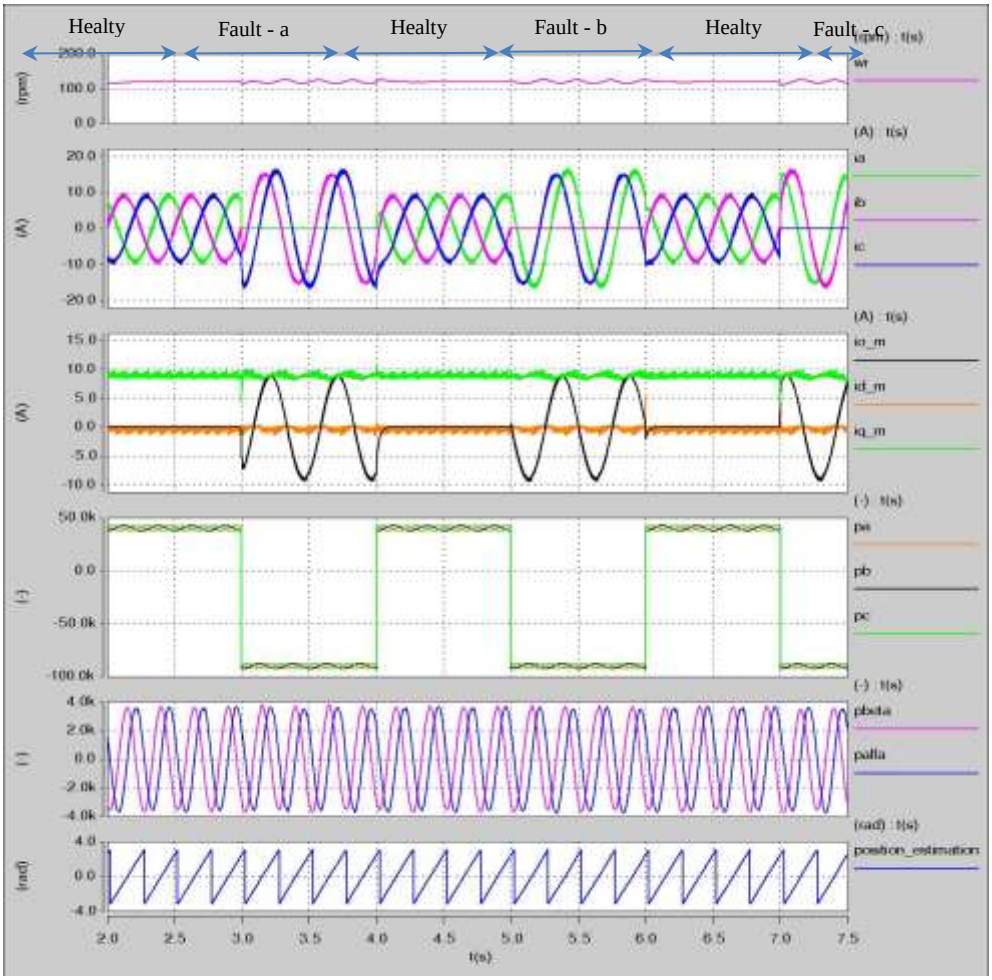

Figure 9. Tracking the Saliency Saturation in Healthy Mode and Open Phase Fault Cases Using the New Algorithm

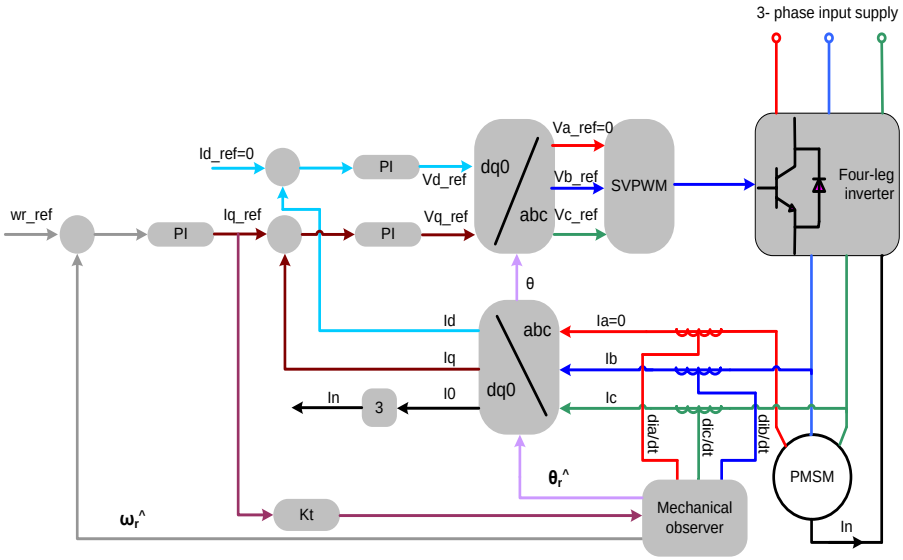

Figure 10. The Sensorless Vector Control Structure for the Four-Phase Inverter PMSM Drive under a Phase 'a' Open-Circuit Fault

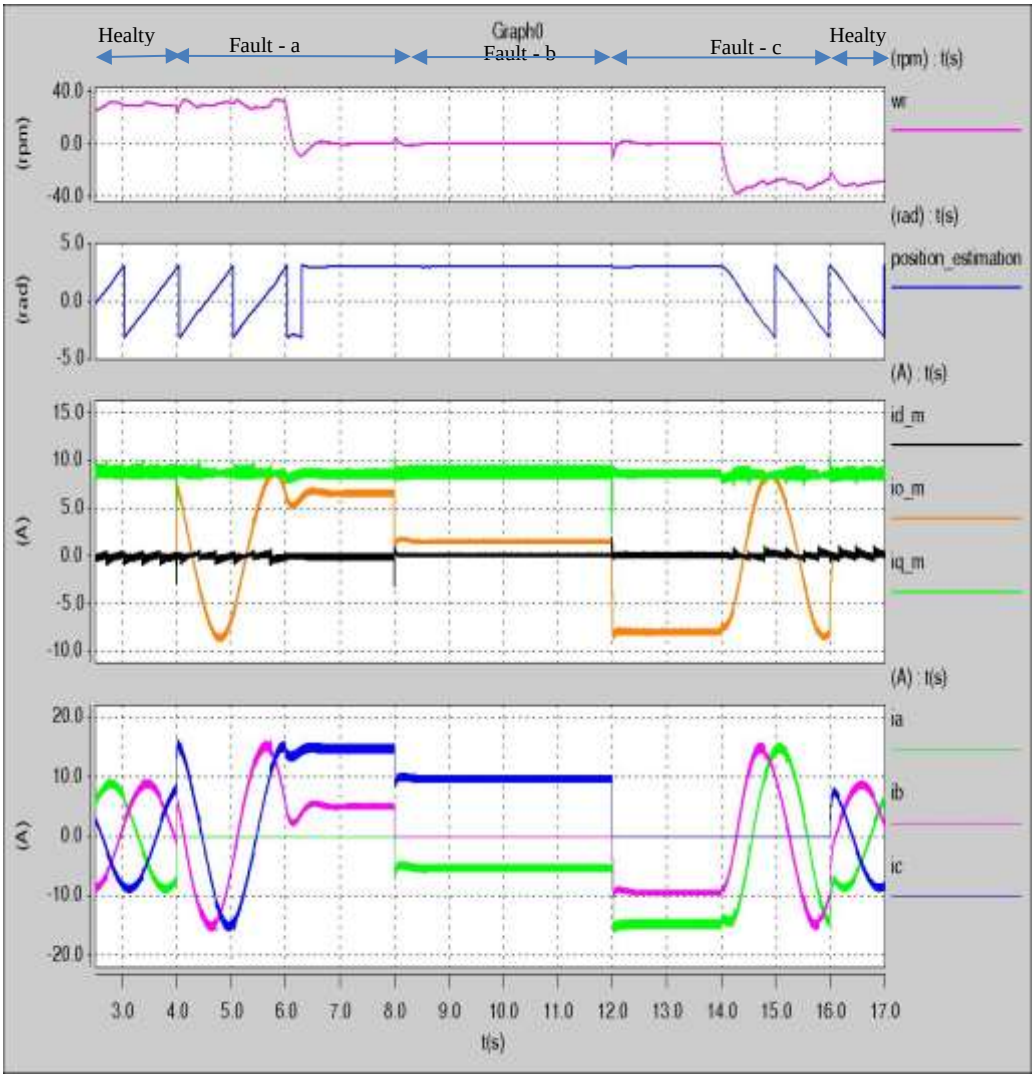

Figure 11. Fully Sensorless Speed Steps between 0.5 Hz,0 to 0.5 Hz half under Healthy Condition and under Open Circuit Fault Conditions

3.2.2 Meduim Speed Operation

Figure 12 shows similar results to those shown in Figure 11 of responding the motor to different fault conditions without affecting the performance of the system but at higher speed steps (6.667 Hz to 0 to -6.667 Hz). The motor was working under healthy conditions at 6.667Hz. At t=3s an open circuit fault in phase ‘a’ is introduced to the system. At t= 4s the fault is removed and the motor returned to work in healthy conditions. At t=4.5s a speed step change from 6.667 Hz to zero is applied to the system. After that at t=5s an open circuit fault is introduced to phase ’b’ till t=6s. Then, the fault in phase ’b’ is removed and the motor retuned to work in healthy conditions again. At t= 6.5 s a speed step change from 0 to -6.667 Hz is applied to the system. And finally, at t=7s an open circuit fault is introduced to phase ‘c’. The system performance during the healthy and unhealthy conditions and during steady state and during transient is excellent.

Figure 13 demonstrate the stability of the fully sensorless system when a load disturbance where applied at speed (8.33 Hz) in both healthy mode and under open phase fault conditions. The motor was working under healthy conditions at no load and at speed 8.33 Hz. At t= 2.5s a load step is applied to the system. After that at t=4s, an open circuit fault is introduced to phase ‘a’. Then, at t=6s the load is removed. at t=8s , the fault is removed from phase ‘a’ and introduced to phase ‘b’. After that at t= 10s, a load step is applied to the system again while the motor under unhealthy conditions. at t=12 s the fault is removed from phase ’b’ and introduced to phase ’c’ and finally at t=14s the load is removed. The results show that the system maintains the speed in all the cases.

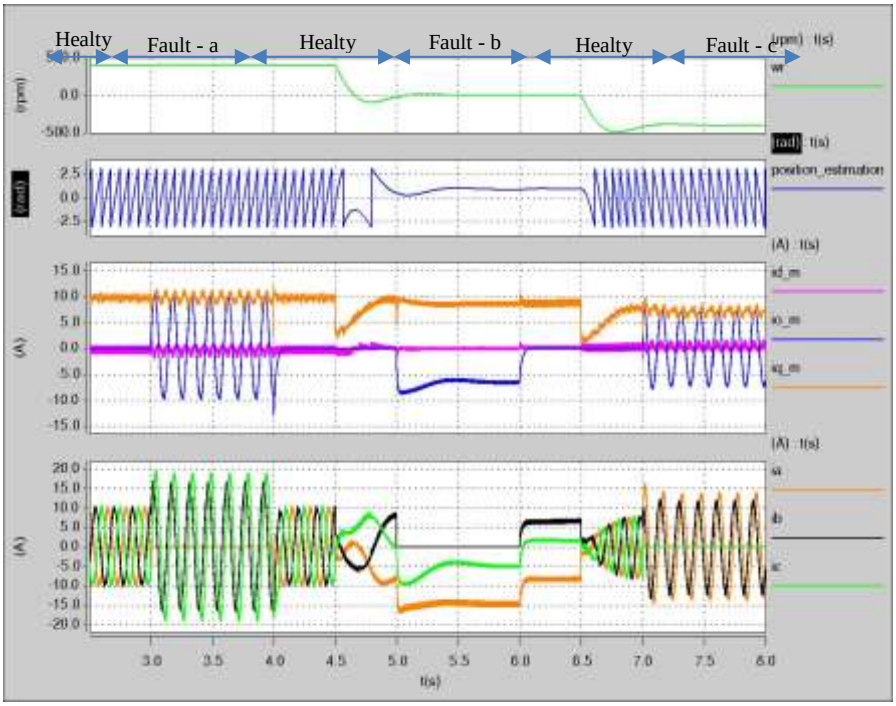

Figure 12. Fully Sensorless Speed Steps between 10 Hz,0 to 10 Hz half under Healthy Condition and under open phase a fault condition

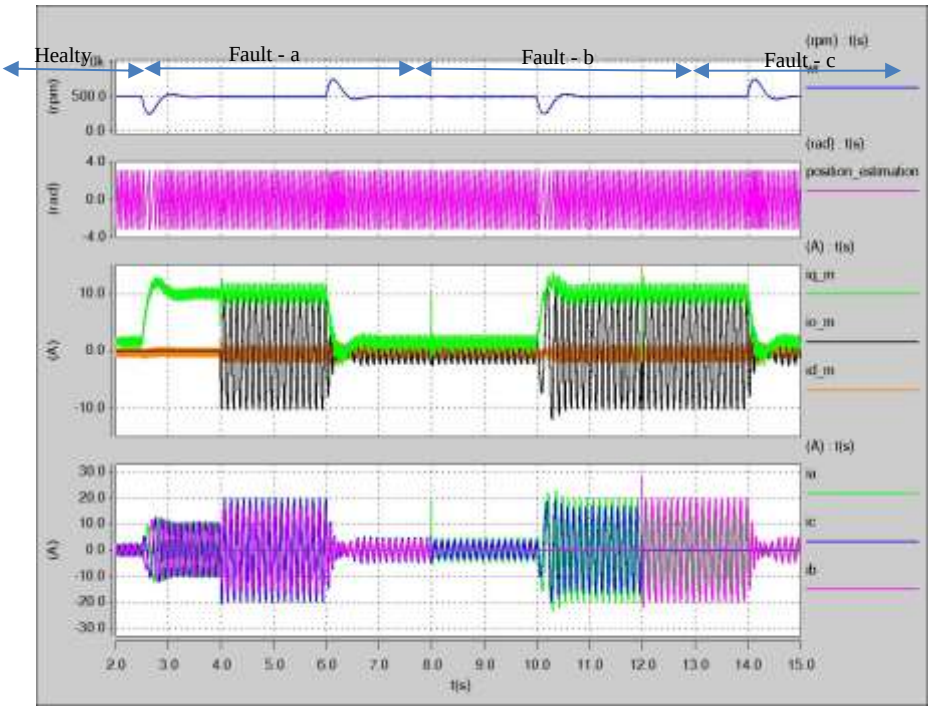

Figure 13. Fully Sensorless Half Load Steps under Healthy Condition and under Open Phase a Fault Condition

4. CONCLUSION

This paper has outlined a new scheme for tracking the saliency of motor fed by a four-leg inverter in case of a single phase open circuit fault through measuring the dynamic current response of the motor line currents due the IGBT switching actions. The proposed method includes software modification to the method

proposed in [6] to track the saliency of the motor under healthy condition to make it applicable in the cases of open circuit phase condition. The new strategy can be used to track the saturation saliency in PM (2 fe) and the rotor slotting saliency in induction motors(14*fr) similar to the method used in healthy motor drive and the only difference between the PM and IM will be the tracked harmonic number. The results have shown the effectiveness of the new method in increasing the safety measures in critical systems needs a continued operation. The drawbacks of this method are increasing the total harmonic distortion of the motors current especially at a very low speed due to the minimum pulse width in addition to the need for 3 di/dt sensors.

APPENDEX

The motor parameters are:- rated speed=2000 rpm, rated torque=10.3 Nm, rated power=2.15 kW, Kt=2 Nm/A, Ke=147.0Vrms/krpm, inertia=20.5 kgcm^2, R(ph-ph)=4 Ω, L(ph-ph)=29.8 mH.

REFERENCES

[1] P.L. Jansen and R.D. Lorenz, "Transducerless position and velocity estimation in induction and salient AC machines", in *IEEE Transactions on Industry Applications*, vol. 31, no. 2, pp. 240-247, Mar/Apr 1995.

[2] Jung-Ik Ha, M. Ohto, Ji-Hoon Jang and Seung-Ki Sul, "*Design and selection of AC machines for saliency-based sensorless control"*, Industry Applications Conference, 2002. 37th IAS Annual Meeting. Conference Record of the, Pittsburgh, PA, USA, 2002, pp. 1155-1162 vol.2.

[3] M. Linke, R. Kennel and J. Holtz, "Sensorless speed and position control of synchronous machines using alternating carrier injection", Electric Machines and Drives Conference, 2003. IEMDC'03. *IEEE International*, 2003, pp. 1211-1217 vol.2.

[4] M. Schroedl, "Sensorless control of AC machines at low speed and standstill based on the "*INFORM" method*", Industry Applications Conference, 1996. Thirty-First IAS Annual Meeting, IAS '96., Conference Record of the 1996 IEEE, San Diego, CA, 1996, pp. 270-277 vol.1.

[5] Juliet and J. Holtz, "*Sensorless acquisition of the rotor position angle for induction motors with arbitrary stator windings"*, Industry Applications Conference, 2004. 39th IAS Annual Meeting. Conference Record of the 2004 IEEE, 2004, pp. 1321-1328 vol.2.

[6] G. Qiang, G. M. Asher, M. Sumner and P. Makys, *"Position Estimation of AC Machines at all Frequencies using only Space Vector PWM based Excitation"*, Power Electronics, Machines and Drives, 2006. The 3rd IET International Conference on, The Contarf Castle, Dublin, Ireland, 2006, pp. 61-70.

[7] A.M.S. Mendes and A.J. Marques Cardoso, "Fault-Tolerant Operating Strategies Applied to Three-Phase Induction-Motor Drives", in *IEEE Transactions on Industrial Electronics*, vol. 53, no. 6, pp. 1807-1817, Dec. 2006.

[8] M.K. Metwally. Control of Four Switch Three Phase Inverter Fed Induction Motor Drives Based Speed and Stator Resistance Estimation. *International Journal of Power Electronics and Drive System (IJPEDS)* Vol. 4, No. 2, June 2014, pp. 192~203

[9] ZMS El-Barbary, HZ Azazi, MK Metwally. Total Harmonic Distortion Analysis of a Four Switch 3-Phase Inverter Fed Speed Sensorless Control of IM Drives. *International Journal of Power Electronics and Drive System (IJPEDS)* Vol. 4, No. 1, March 2014 pp. 81~90 ISSN: 2088-8694

[10] N. Bianchi, S. Bolognani, M. Zigliotto and M. Zordan, "Innovative remedial strategies for inverter faults in IPM synchronous motor drives", in *IEEE Transactions on Energy Conversion*, vol. 18, no. 2, pp. 306-314, June 2003.

[11] F. Meinguet and J. Gyselinck, "*Control strategies and reconfiguration of four-leg inverter PMSM drives in case of single-phase open-circuit faults"*, Electric Machines and Drives Conference, 2009. IEMDC '09. IEEE International, Miami, FL, 2009, pp. 299-304.

[12] S. Kwak, T. Kim and O. Vodyakho, *"Four-leg based Matrix Converter with Fault Resilient Structures and Controls for Electric Vehicle and Propulsion Systems*", 2007 IEEE Vehicle Power and Propulsion Conference, Arlington, TX, 2007, pp. 519-523

[13] Saleh K, Sumner M. Modelling and simulation of a sensorless control of four-leg inverter PMSM drives in case of single-phase open circuit fault. *TURKISH JOURNAL OF ELECTRICAL ENGINEERING & COMPUTER SCIENCES*. 2016

[14] B.A. Welchko, T.A. Lipo, T.M. Jahns and S.E. Schulz, "Fault tolerant three-phase AC motor drive topologies: a comparison of features, cost, and limitations", in *IEEE Transactions on Power Electronics*, vol. 19, no. 4, pp. 1108-1116, July 2004.

[15] S. Khwan-on, L. de Lillo, P. Wheeler and L. Empringham, "Fault tolerant four-leg matrix converter drive topologies for aerospace applications", 2010 *IEEE International Symposium on Industrial Electronics*, Bari, 2010, pp. 2166-2171.

[16] A. Gaeta, G. Scelba and A. Consoli, "Modeling and Control of Three-Phase PMSMs Under Open-Phase Fault", in *IEEE Transactions on Industry Applications*, vol. 49, no. 1, pp. 74-83, Jan.-Feb. 2013.

[17] B. Mirafzal, "Survey of Fault-Tolerance Techniques for Three-Phase Voltage Source Inverters", in *IEEE Transactions on Industrial Electronics*, vol. 61, no. 10, pp. 5192-5202, Oct. 2014.
[18] J. Viola, F. Quizhpi, J. Restrepo, J.P. Pesántez and M.M. Sánchez, "*Analysis of a four-phase induction machine with direct torque control*", Power Electronics and Applications (EPE), 2013 15th European Conference on, Lille, 2013, pp. 1-9..
[19] K. Nguyen-Duy, T.H. Liu, D.F. Chen and J.Y. Hung, "Improvement of Matrix Converter Drive Reliability by Online Fault Detection and a Fault-Tolerant Switching Strategy", in *IEEE Transactions on Industrial Electronics*, vol. 59, no. 1, pp. 244-256, Jan. 2012.
[20] R.D. Lorenz and K.W. Van Patten, "High-resolution velocity estimation for all-digital, AC servo drives", in *IEEE Transactions on Industry Applications*, vol. 27, no. 4, pp. 701-705, Jul/Aug 1991.

BIOGRAPHIES OF AUTHORS

Kamel Saleh received the B.Eng degree in Electrical and Electronic Engineering from An-Najah National University in 2003 and then worked at Palestinian Ministry of Energy for two years. Moving to the University of Nottingham, he completed his master degree and PhD in Electrical drives in 2010. After working as a research assistant at Nottingham university, he was appointed as a Lecturer at An-Najah National University in 2011. He is now assistant professor of Electrical Engineering dept. His research interests cover control of power electronic systems including sensorless motor drives, diagnostics and prognostics for drive systems, power electronics for enhanced power.

Mark Sumner received the B.Eng degree in Electrical and Electronic Engineering from Leeds University in 1986 and then worked for Rolls Royce Ltd in Ansty, UK. Moving to the University of Nottingham, he completed his PhD in induction motor drives in 1990, and after working as a research assistant, was appointed Lecturer in October 1992. He is now Professor of Electrical Energy Systems. His research interests cover control of power electronic systems including sensorless motor drives, diagnostics and prognostics for drive systems, power electronics for enhanced power quality and novel power system fault location strategies.